Materials Science-Poland, 34(1), 2016, pp. 13-18
http://www.materialsscience.pwr.wroc.pl/
DOI: 10.1515/msp-2016-0013

DE GRUYTER OPEN

Influence of Ta_2O_5 doping on mechanical and biological properties of silicate glass-ceramics

MADEEHA RIAZ[1]*, REHANA ZIA[1], FARHAT SALEEMI[2], FAROOQ BASHIR[1], RIAZ AHMAD[3], TOUSIF HOSSAIN[3]

[1]Department of Physics, Lahore College for Women University, Lahore, Pakistan

[2]Government College for Women University, Sialkot, Pakistan

[3]CASP, Government College University, Lahore, Pakistan

The mechanical properties of silicate glass-ceramics were evaluated based on the compressive strength tests. It was found that Ta_2O_5 addition improved densification, refinement of the microstructure and toughening of the bodies. The maximum compressive strength of the bodies with 1 mol% Ta_2O_5 was increased 3-fold (245.92 ±0.3 MPa) in comparison to undoped glass-ceramics which was measured to be 89.04 ±0.3 MPa, while for 3 mol% it became 4-fold (387.12 ±0.4 MPa) greater. The addition of Ta_2O_5 stabilized the system by controlling the biodegradation of the glass-ceramics. It effectively depressed the apatite formation as by addition of 3 mol% Ta_2O_5 no apatite layer was observed. It may be concluded from this study that mechanical and physical properties can be improved by the addition of Ta_2O_5, but at a cost of bioactivity. Still the optimized composition having $Ta_2O_5 \leqslant 1$ mol% may provide appropriate strength of biomaterials for high load bearing applications.

Keywords: *compressive strength; bioactivity; Ta_2O_5; glass-ceramics*

1. Introduction

Glass-ceramics are polycrystalline solids, partially crystalline and partially amorphous. Due to the presence of both crystalline and residual glassy phase, glass-ceramics possess a combination of valuable properties of both glasses and ceramics [1]. Glass-ceramics have gain importance in recent years due to their remarkable dielectric, structural, mechanical [2] and biocompatible properties [3] which find application in various fields of telecommunication [4], architecture [5], and health care [6]. The physical and chemical properties of glass-ceramics mainly depend on the composition of glass, type and amount of the crystalline phase, microstructure, the heat treatment procedure and nucleating agents [7]. Glass-ceramics are also considered as intrinsic composites because during heat treatment the reinforcing phase is nucleated from the parent glass, which, therefore, provides toughness and mechanical strength to the polycrystalline solid [8]. Previously a number of studies have been made on doped glass-ceramics with different nucleating agents, such as TiO_2, ZrO_2, P_2O_5, Y_2O_3, CeO_2, Fe_2O_3, Cr_2O_3, NiO, ZnO and V_2O_5 [9, 10], to obtain effective crystallization and sinterability of the glass-ceramics. Naga et al. [11] reported that doping of Ta_2O_5 improved densification, hardness and toughness of pure alumina. It was stated that mechanical strength can be enhanced with addition of Ta_2O_5 to bioactive material 45S5Bioglass®, the most extensively studied material that has both osteoconductive and osteoproductive abilities, so that it may be used for high load bearing applications [12]. Furthermore, even a small amount of Ta_2O_5 inhibits bone bonding [13]. The present study aims to optimizing properties and investigating the effectiveness of Ta_2O_5 on the structural and biological characteristics of SiO_2–CaO–Na_2O–P_2O_5 (45S5) glass-ceramics.

2. Experimental

2.1. Sample preparation

Five different batches of composition $(46.1-x)SiO_2$–$(x)Ta_2O_5$–(26.9)CaO–$(24.4)Na_2O$––$(2.6)P_2O_5$, where x = 0, 0.1, 0.5, 1.0, 3.0 (mol%)

*E-mail: madeehariaz2762@yahoo.com

illustrated in Table 1, were melted at 1500 °C in a Pt crucible for 2 hours and the melt was quenched in water and dried. The obtained glass frits were subsequently dry-crushed in an agate mortar and pestle for several hours and then sieved to yield a powder measuring <40 μm in particle size. Thereafter, the powder was compacted into 15 mm in diameter and 4 mm thickness disc shaped pellets under hydrostatic pressure of 48 MPa. The glass compacts were sintered for four hours at crystallization peak temperature 'T_c' (given in Table 1), corresponding to the exothermic peaks from Differential Scanning Calorimetric (SDT-Q600 Thermal Analyzer) curves shown in Fig. 1.

2.2. Structural and mechanical characterization techniques

The microstructural characterization of the sample was performed by X-ray diffraction method – XRD (Bruker D8 Discover Diffractometer) – using CuKα radiation (λ = 1.54056 Å) in 20 to 40° 2θ range and the data were evaluated by JCPDS reference data. Archimedes principle was applied to study the densification behavior of the samples. Morphological examination of the samples was performed by scanning electron microscope – SEM (JSM-6480 LV, JEOL) – at an accelerating voltage of 15 kV, using a secondary mode of imaging. Mechanical properties of the specimens were evaluated by electronic universal tester (INSTRON, model 3384) having maximum load capacity of 150 kN. For compression strength tests, specimens with circular shape, having 15 mm in diameter and 4 mm thickness were used; the load was applied at a crosshead speed of 0.5 mm/min till the fracture point.

2.2.1. *In vitro* bioactivity assays

The assessment of *in vitro* bioactivity of the samples in the present study was carried out in Kokubo's SBF [14] with ion concentration nearly similar to human blood plasma for thirty days at 37 °C in static conditions and 0.1 cm^{-1} SA/V ratio was maintained for all immersed samples. XRD and SEM-EDX were used for *in vitro* characterization.

3. Result and discussion

3.1. Differential scanning calorimetric analysis

The differential scanning calorimetric results depicted in Fig. 1 illustrate that with increasing amount of Ta_2O_5 in SiO_2–CaO–Na_2O–P_2O_5 (45S5) glass-ceramic system from 0 to 3 mol%, both glass transition and crystallization temperature decrease. The nucleating agent enhances the tendency of crystallization by creating heterogeneous nucleating sites either by precipitation of the nucleating agent or phase separation creating separated and non-bridging oxygen ions that in turn decrease the viscosity of the melt, which results in an increase of crystallization ability of the glasses [9, 15]. The DSC results collected in Table 1 indicate that Ta_2O_5 was effective in inducing crystallization, thus, enhancing crystallization of the glass. The possible reason for this result is that Ta^{+5} ions have high field strength which increases phase separation in the glass and alters the basic structural unit; hence, enhancing the tendency to crystallization of the glass.

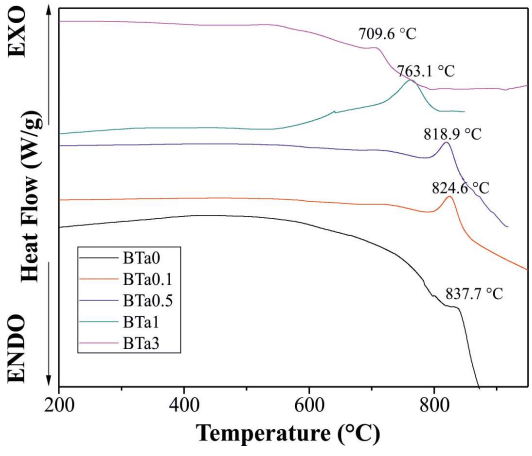

Fig. 1. The DSC thermogram of tantalum based glass-ceramics showing crystallization temperature (T_c).

3.2. X-ray diffraction analysis

The X-ray diffraction (XRD) patterns in Fig. 2 show the presence of different crystalline phases. The peaks can be ascribed to

Table 1. Glass transition temperature T_g and crystallization temperature T_c.

Sample ID	Chemical composition (mol%)	Glass transition temperature [T_g] °C	Crystallization temperature [T_c] °C
Ta0	$46.1SiO_2$–$0Ta_2O_5$–$26.9CaO$–$24.4Na_2O$–$2.6P_2O_5$	546.9	837.7
Ta0.1	$46.0SiO_2$–$0.1Ta_2O_5$–$26.9CaO$–$24.4Na_2O$–$2.6P_2O_5$	540.1	824.6
Ta0.5	$45.6SiO_2$–$0.5Ta_2O_5$–$26.9CaO$–$24.4Na_2O$–$2.6P_2O_5$	506.8	818.9
Ta1	$45.1SiO_2$–$1Ta_2O_5$–$26.9CaO$–$24.4Na_2O$–$2.6P_2O_5$	449.4	763.1
Ta3	$43.1SiO_2$–$3Ta_2O_5$–$26.9CaO$–$24.4Na_2O$–$2.6P_2O_5$	312.4	709.6

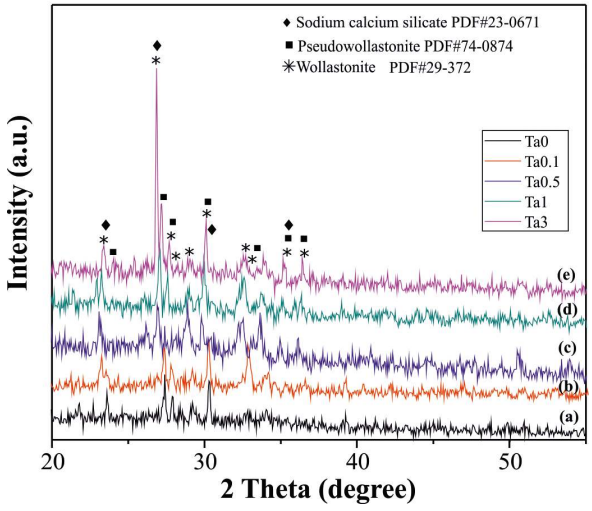

Fig. 2. Comparative X-ray diffraction patterns of (a) Ta0, (b) Ta0.1, (c) Ta0.5, (d) Ta1, (e) Ta3 glass-ceramics (■ – pseudowollastonite (α-$Ca_3(Si_3O_9)$); * – wollastonite ($CaSiO_3$); ♦ – sodium calcium silicate ($Na_2Ca_3Si_6O_{16}$).

wollastonite ($CaSiO_3$, PDF#029-372), pseudowollastonite (α-$Ca_3(Si_3O_9)$, PDF#01-074-0874) and sodium calcium silicate ($Na_2Ca_3Si_6O_{16}$, PDF#023-0671). Wollastonite is the main crystalline phase present in all the samples. The results show an increase in intensity of the peaks with the addition of small concentration of Ta_2O_5 (0.1 to 3) mol%, indicating crystal growth. The crystalline phases in heat treated samples show a slight phase shift, which originats from internal stresses caused by the lattice distortion [15] due to addition of Ta_2O_5 nucleating agent. The sample having 0 mol% Ta_2O_5 shows the lowest crystallization, while the one having 3 mol% Ta_2O_5 displays much more enhanced crystallization, which is confirmed by the strongest crystallization peaks observed in the XRD patterns. The enhancement of crystalline phases with increasing amount of Ta_2O_5 is due to the fact that the oxides of transition metals increase the trend towards separation of phases, hence, enhance crystallization [16]. The average crystallite size of wollastonite main phase is calculated by Scherrer's formula:

$$t = K\lambda / B\cos\theta \tag{1}$$

where K = 1 is shape constant, $\lambda = 0.154056$ nm is the wavelength of incident X-ray, B is full width half maximum (FWHM) of a particular diffraction peak, θ is Bragg's angle of diffraction peak. The average crystallite size (Fig. 3) increased uniformly with the progressive addition of Ta_2O_5 (from 0 to 3 mol%), indicating the growth of the crystal.

3.3. Morphological characterization

Scanning electron micrograph in Fig. 4 shows the surface morphologies of Ta0, Ta0.1, Ta0.5, Ta1 and Ta3 as-sintered samples. The SEM in Fig. 4a of the sample Ta0 shows irregular shaped crystals embedded in the glassy matrix. Small pits and cuts observed on the surface indicate low microhardness suggesting low mechanical strength, which was also confirmed by the compressive strength measurements. SEM in Fig. 4b of sample Ta0.1 reveals small globular shaped crystals spreaded all over the surafce along with some larger crystals.

The pits are noticeably reduced with the addition of 0.1 mol% Ta_2O_5 indicating improvement in mechanical strength of the material though a few pores and cracks are also observed. The larger

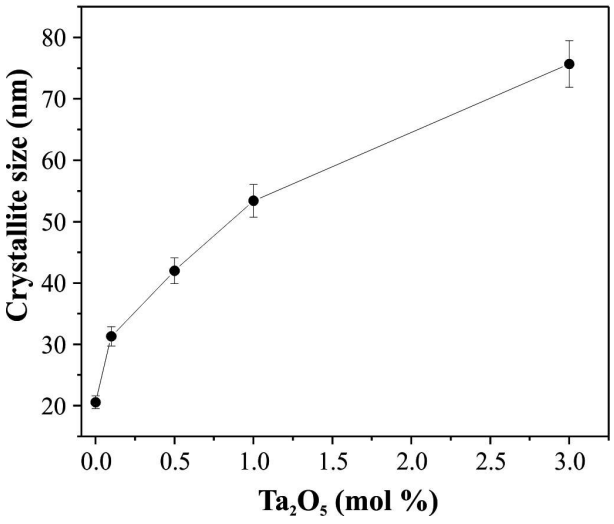

Fig. 3. Change in crystallite size with Ta_2O_5 concentration using Scherer's formula.

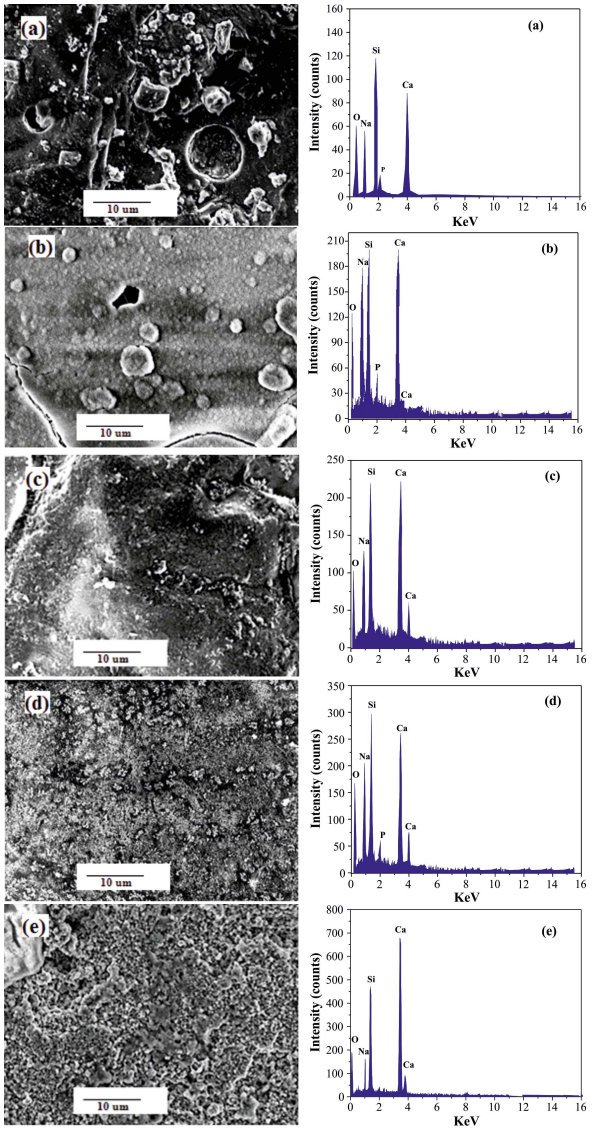

Fig. 4. SEM micrographs of surfaces of glass-ceramics (a) Ta0, (b) Ta0.1, (c) Ta0.5, (d) Ta1 and (e) Ta3, respectievly.

sized grains observed in Fig. 4a and 4b are of psedowollastonite type in accordance with XRD results. These grains have been decomposed with the increase in concentration of Ta_2O_5 >0.1 mol% in the system, as shown in Fig. 4c of the sample Ta0.5, where only small size grains scattered throughout are observed. This result is in agreement with the XRD findings. The surface morphology of Ta0.5 sample shows the diffusion of particles along the grain boundaries, causing the vacancy annihilation, ellimination of the porosity and coalescence of particles, significantly enhancing the density as well as mechanical strength of the material. The SEM in Fig. 4d of sample Ta1 displays small crystals spread all over the surface along with few agglomerates dispersed. The SEM in Fig. 4e of sample Ta3 shows coalescence of agglomerates, reduction of porosity and the most densely packed structure. Fig. 5 shows that with an increase in concentration of Ta_2O_5 from 0 to 3 mol% the grain size decreased from 4.76 to 1.92 μm and pore size reduced to 0.39 μm.

3.4. Physical properties

Fig. 6 depicted that with a rise in apparent density of the glass-ceramics the compressive strength also increased. This result is attributed to reduction in porosity and refinement of microstructure; in the microstructure the size of crystals has the utmost importance in preventing the propagation of cracks in the whole structure. According to the Hall-Petch effect, as the grain size decreases the strength and toughness of the material increases; generally it can be said that fine grain size strengthens the material. The effect of incorporation of Ta_2O_5 on the apparent density of the samples (Fig. 6), indicates that increasing the content of dopant (Ta_2O_5) enhances

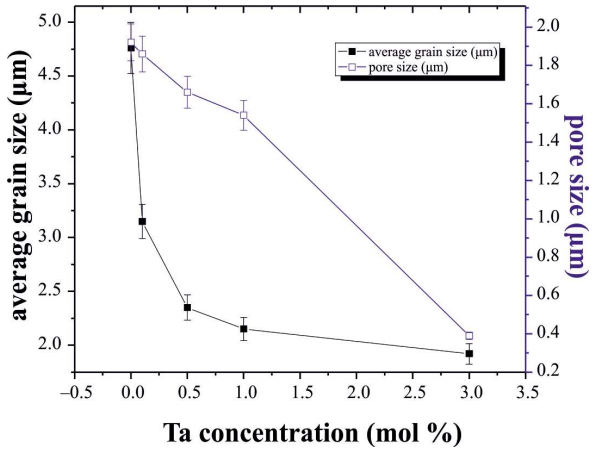

Fig. 5. The variation of grain size and porosity with change in Ta_2O_5 concentration (mol%).

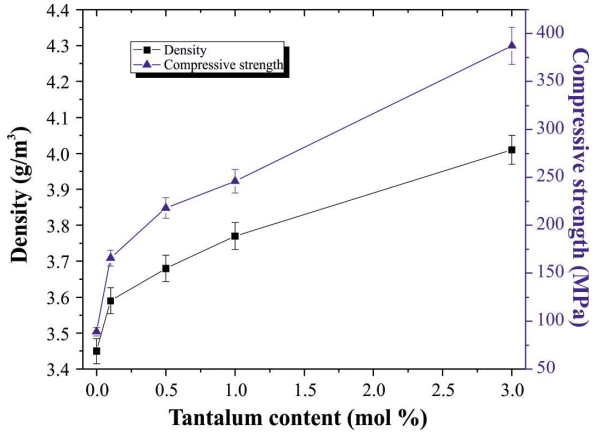

Fig. 6. Apparent density and compressive strength as function of Ta_2O_5 concentration in mol%.

the apparent density. It may be assumed that small ionic radius (0.7 Å) of dopant Ta is responsible for acceleration of densification process, as it is well known that the smaller the ionic radius of dopant the better the densification rate [11]. An enormous rise in apparent density was observed when Ta_2O_5 dopant increased to 3 mol%, Ta3 glass-ceramic showed superior density among others, indicating the reduction of pores and diffusion of particles along the grain boundaries.

3.5. *In vitro* analysis

Fig. 7 shows the XRD patterns of the surfaces of the glass-ceramics after soaking in SBF for 30 days. For the glass-ceramics Ta0, sharp peaks of HCAp ($(Ca_{10}(PO_4{\cdot}CO_2OH_6)(OH)_2)$, PDF#04-0697) at 22.79° and 33.03° indicate well crystallized apatite layer on the sample surface, which is in accordance with the SEM image in Fig. 8. Addition of Ta_2O_5 into the system caused suppression of the apatite formation, the broad HCAp peaks and reduction in width and intensity of 22.79° and 33.03° peaks, indicating low crystallinity and small crystal size. The Ta1 glass-ceramics shows a broad diffraction peak corresponding to HCAp crystallized peaks at 2θ ranging from 31° to 38°. No HCAp peaks are observed for Ta3 glass-ceramics.

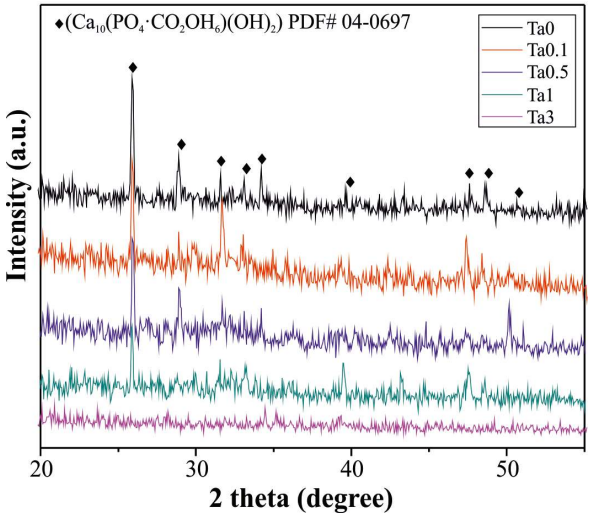

Fig. 7. The XRD patterns for (a) Ta0, (b) TA0.1, (c) Ta0.5, (d) Ta1 and (e) Ta3 glass-ceramics after 30-day immersion in Stimulated Body Fluid (SBF).

Fig. 8 shows the SEM micrographs of all glass-ceramics samples soaked in SBF for 30 days. The apatite layer fully covered the surface of the sample Ta0 indicating high degree of bioactivity, but with addition of Ta_2O_5 the bioactivity decreased, which is in agreement with the findings of Imayoshi et. al. [17] that addition of Ta_2O_5 to $CaO{\cdot}SiO_2$ based glass suppressed the rate of apatite formation. No continuous apatite layer was formed after 30 days of immersion in SBF solution, a few apatite crystal precipitates were detected on the surface of the glass-ceramics. The apatite layer has not formed on the Ta3 glass-ceramics which is in agreement with

the phase analysis (Fig. 7). The XRD and SEM-EDX results confirm the presence of apatite layer only on the surfaces of the glass-ceramics having Ta_2O_5 concentration less than 3 mol%.

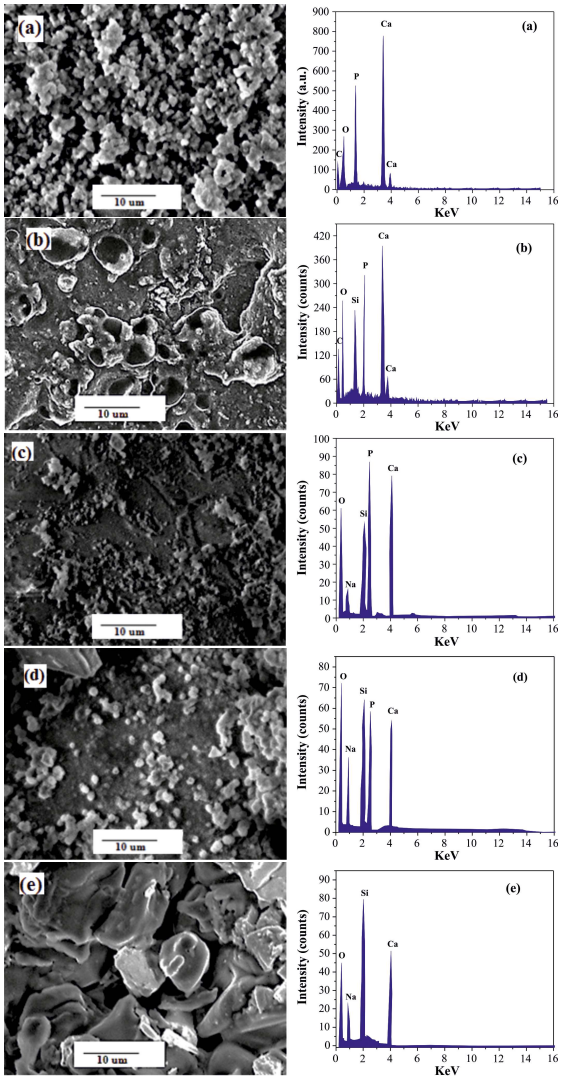

Fig. 8. SEM-EDX micrographs of surfaces of glass-ceramics (a) Ta0, (b) Ta0.1, (c) Ta0.5, (d) Ta1 and (e) Ta3 after soaking in SBF for 30 days.

4. Conclusions

The incorporation of Ta_2O_5 in the 45S5 glass-ceramic system shifted both nucleation and crystallization temperature to lower values and acted as a nucleating agent in the system, decreasing the viscosity and increasing the tendency to glass crystallization. The apparent density and degree of crystallization was also enhanced with Ta_2O_5 addition, which consequently improved the compressive strength of the ceramics derivatives. The *in vitro* analysis studies on SiO_2–CaO–Na_2O–P_2O_5 glass-ceramics containing 0.1 to 2 mol% Ta_2O_5 showed that these glass-ceramic materials are capable of bonding with the natural human bone. It may be concluded that a small content of Ta_2O_5 can effectively enhance the crystallization, mechanical strength and control the biodegradation of the glass-ceramics to make it suitable for high load bearing applications.

References

[1] HASHMI M.U., SHAH S.A., UMER F., ALKEDY A.S., *Ceram. Silik.*, 57 (4) (2013), 313.
[2] BEALL G.H., *J. Euro. Ceram. Soc.*, 29 (2009), 1211.
[3] SINGH R.K., KOTHIYAL G.P., SRINVASAN A., *J. Appl. Surf. Sci.*, 255 (2009), 6827.
[4] MARQUES V.M.F., TULYAGANOV D.U., KOTHIYAL G.P., FERREIRA J.M.F., *J. Electroceram.*, 25 (2010), 38.
[5] ZHAOA Y., CHENA D., BIB Y., LONGA M., *Ceram. Int.*, 38 (3) (2012), 2495.
[6] ELBATAL H.A., KHALIL E.M.A., HAMDY Y.M., *Ceram. Int.*, 35 (2009), 1195.
[7] GUO X., YANG H., *J. Non-Cryst. Solids*, 351 (2005), 2133.
[8] BERTAN F.M., NOVAES DE OLIVEIRA A.P., MONTEDO O.R.K., HOTZA D., RAMBO C.R., *Cerâmica*, 59 (2013), 351.
[9] REZVANI M., *Iran. J. Sci. Technol.*, 7 (4) (2010), 8.
[10] REZVANI M., *Iran. J. Sci. Technol.*, 8 (4) (2011), 41.
[11] NAGA S.M., HASSAN A.M., AWAAD M., BONDIOLI F., *Ceram. Sci. Tech.*, 04 (4) (2013), 187.
[12] DOROZHKIN S.V., *Biomaterials*, 1 (1) (2011), 3.
[13] RATNER B.D., HOFFMAN A.S., SCHOEN F.J., LEMONS J.E. (Eds.), *Biomaterials Science: An Introduction to Materials in Medicine*, 3rd ed., Academic Press, 1996.
[14] KOKUBO T., TAKADAMA H., *Biomaterials*, 27 (2006), 2907.
[15] LIU H., WANG Y., WANG T., YANG R., LIU S., *Ceram. Int.*, 40 (2014), 453.
[16] HUDON P., BAKER D.R., *J. Non-Cryst. Solids*, 303 (2002), 299.
[17] IMAYOSHI N., OHTSUKI C., HAYAKAWA S., OSAKA A., *Mem. Sch. Eng. Okayama Univ.*, 31 (2) (1997), 39.

Received 2015-01-17
Accepted 2015-11-23